Science in China Series E: Technological Sciences

www.scichina.com
tech.scichina.com
www.springerlink.com

Synchronous estimation of DTM and fractional vegetation cover in forested area from airborne LIDAR height and intensity data

BAO YunFei[1,2], CAO ChunXiang[1†], ZHANG Hao[1], CHEN ErXue[3], HE QiSheng[1,2], HUANG HuaBing[1], LI ZengYuan[3], LI XiaoWen[1,4] & GONG Peng[1]

[1] State Key Laboratory of Remote Sensing Science, jointly sponsored by the Institute for Remote Sensing Applications of Chinese Academy of Sciences and Beijing Normal University, Beijing 100101, China;
[2] Graduate University of the Chinese Academy of Sciences, Beijing 100049, China;
[3] Institute of Forest Resource Information Technique, the Chinese Academy of Forestry, Beijing 100091, China;
[4] Research Center for Remote Sensing and GIS, Department of Geography and Beijing Key Laboratory for Remote Sensing of Environment and Digital Sites, Beijing Normal University, Beijing 100875, China

We proposed a method to separate ground points and vegetation points from discrete return, small footprint airborne laser scanner data, called skewness change algorithm. The method, which makes use of intensity of laser scanner data, is especially applicable in steep, and forested areas. It does not take slope of forested area into account, while other algorithms consider the change of slope in steep forested area. The ground points and vegetation points can be used to estimate digital terrain model (DTM) and fractional vegetation cover, respectively. A few vegetation points which were classified into the ground points were removed as noise before the generation of DTM. This method was tested in a test area of 10000 square meters. A LiteMapper-5600 laser system was used and a flight was carried out over a ground of 700—800 m. In this tested area, a total number of 1546 field measurement ground points were measured with a total station TOPCON GTS-602 and TOPCON GTS-7002 for validation of DTM and the mean error value is –18.5 cm and the RMSE (root mean square error) is ±20.9 cm. A data trap sizes of 4 m in diameter from airborne laser scanner data was selected to compute vegetation fraction cover. Validation of fractional vegetation cover was carried out using 15 hemispherical photographs, which are georeferenced to centimeter accuracy by differential GPS. The gap fraction was computed over a range of zenith angles 10° using the gap light analyzer (GLA) from each hemispherical photograph. The R^2 for the regression of fractional vegetation cover from these ALS data and the respective field measurements is 0.7554. So this study presents a method for synchro-

Received September 29, 2008; accepted December 31, 2008
doi: 10.1007/s11431-008-6018-x
†Corresponding author (email: cao413@irsa.ac.cn)
Supported by the National State Key Basic Research Project (Grant No. 2007CB714404), the National Natural Science Foundation of China (Grant No. 40871173), the State Key Laboratory of Remote Sensing Science, China (Grant No. 03Q0030449) and Key Science and Technology R&D Program of Qinghai Province (Grant No. 2006-6-160-01)

nous estimation of DTM and fractional vegetation cover in forested area from airborne LIDAR height and intensity data.

LIDAR, intensity, skewness, synchronous, DTM, fractional vegetation cover

1 Introduction

Airborne laser scanning data have been widely used to retrieve the forest structure parameters. Generation of digital terrain model (DTM) in forested area is very important for estimation of canopy height and fractional cover describing vegetation cover density which serves as an important parameter for biosphere modeling[1, 2]. In forested area, DTM can be generated from ground points of lidar data and fractional cover can be derived from vegetation points of lidar data. Separation of ground points and above-ground points is a significant work for retrieval of forest structure information during the processing of LIDAR data. In previous studies, different algorithms had been developed for generation of DTM from airborne laser scanning data. An interpolated surface was fitted to the lidar data to filter out trees in forested areas and an iterative least-squares algorithm was used to reduce the contribution of points above the surface[3]. Ground points were derived from non-ground points by iterative threshold-dependent densification of a triangulated irregular network (TIN) for derivation of DTM[4]. As a means of image processing, morphological filtering was firstly used to remove the contribution of non-ground points from lidar data[5]. Then different kinds of morphological filtering algorithms have been also developed for distinguishing terrain from non-terrain LIDAR points. Height differences between ground points were used to determine the optimal filtering function[6]. Based on the assumption that the slope is constant, a progressive morphological filter was developed to remove non-ground points by gradually increasing the window size of the filter and using elevation difference thresholds[7], while a new morphological filtering algorithm was presented, which did not require the assumption[8]. In addition to these methods, other algorithms have been developed in recent years[9−12]. A statistical method——skewness balance was used to separate object and ground points based on height information of high-resolution lidar data[13]. Height and intensity information of lidar were simultaneously used to separate vegetation points from ground points in forested area[14], since the statistical method using only height information was not successful in forested area with slope terrain.

There are two kinds of methods for the retrieval of fractional vegetation cover from passive optical images, including regression models[15,16] and radiative transfer modeling[17,18]. The limited characterization of canopy structure in both horizontal and vertical dimensions is one of the limitations of these methods[19]. Airborne laser scanning data have been proved to provide high precise vegetation structure information[20−26]. Some studies have derived fractional cover from laser scanning. Fractional cover was estimated using height cutoff from Laser altimeter[27]. Two methods were used to calculate the fractional cover [28]. The first method classified the first and last returns from the same laser shot and the second used the lidar intensity to measure the proportion of the canopy hits while the percentage of canopy hits was calculated for fractional cover, assuming that all laser pulses within a height less than 3 m were understory and ground hits[29]. The fractional cover was estimated from the first return of lidar data since a multiple regression of fractional cover derived from the first and last returns with field data showed no enhancement compared to the regression of the first return[19]. Additionally, an LIDAR waveform model was developed to re-

trieve fractional cover from large footprint lidar data[30].

As seen from previous studies, both DTM and fractional cover can be better retrieved by accurately separating vegetation points from ground points. Derivation of fractional cover from airborne laser scanning data requires complete vegetation points above ground while generation of DTM from lidar data requires no above-ground points. As for the laser scan system recording discrete returns, it is difficult to separate the two kinds of points from total lidar data by the order of discrete returns or height above ground, especially in sloped area. The objective of this study is to classify ground points and vegetation points from lidar height and intensity information and synchronously derive DTM and vegetation fractional cover. Our aim is to explore the intensity information of lidar data and explain the theory of separation based on the basic measuring principle of laser scanning.

2 Data

2.1 Study site

The forested area used in this study is located in Qilian Mountain, northwest China. The locations of the field measurements are largely dominated by Qinghai spruce (*P.crassifolia*), which may be used as important indicator plant of the environmental change of the mountain area of the upriver region of the Heihe River.

2.2 Laser scanning data

An airborne laser scan flight was carried out over the test area in June 2008. The airborne laser scan system used was LiteMapper-5600 developed by the German company IGI. It is one of the first commercial airborne LIDAR terrain mapping systems to use waveform digitization. Its laser scanner is RIEGL LMS-Q560. The sensor specifications are given in Table 1.

Table 1 Specifications of RIEGL LMS-Q560

RIEGL LMS-Q560	
Max. Measurement range	1800 m
Measurement accuracy	20 mm
Max. Pulse repetition frequency	200 kHz
Multiple target separation within single shot	0.6 m
Laser wavelength	1550 nm
Return pulse width resolution	0.15 m
Scan speed	10－160 scan/s
Scan angle accuracy	0.001°
Laser beam divergence	0.5 mrad

The flight over our study area was conducted with a nominal height over ground of 700－800 m, leading to a point density of 0.36－1.6 points per square meter. For increasing the point density, repetitive flight was carried out over the same study area. The flights in our study area are 5 times more than those in other areas, so the point density was increased to 2－7 points per square meter. Additionally, as the laser scanner records a waveform data, multiple returns need to be sampled from the waveform data for our algorithm in this study.

2.3 Field inventory

For performance evaluation of DTM from the algorithm in this study, five points were measured with GPS Z-MAX and elevations of the ground points in the forested area were established from two points of these points. A total number of 1546 field measured ground points were measured with a total station TOPCON GTS-602 and TOPCON GTS-7002 with accuracy ± 2 mm. Applying error propagation, the accuracy of these points is estimated as ± 8 cm in either coordinate direction. Because the average of slope in the forest area is about 10°, the height error from total station amounts to ± 8.7 cm.

We took hemispherical photographs as field samples using Nikon Coolpix 8400 with FC-E9 adapter lens. The measurements were performed under overcast conditions to minimize the effect of the sky radiance on the digital image. In Figure 1, black dots indicate positions where hemispherical photographs were taken in June 2008. A total of 15 hemispherical photographs were taken and their locations were measured using differential GPS equipment. The hemispherical photographs were analyzed using the gap light analyzer software[31]. Gap fractions were computed for zenith angles 0°—90° with the interval of 5° and averaged over all azimuth angles.

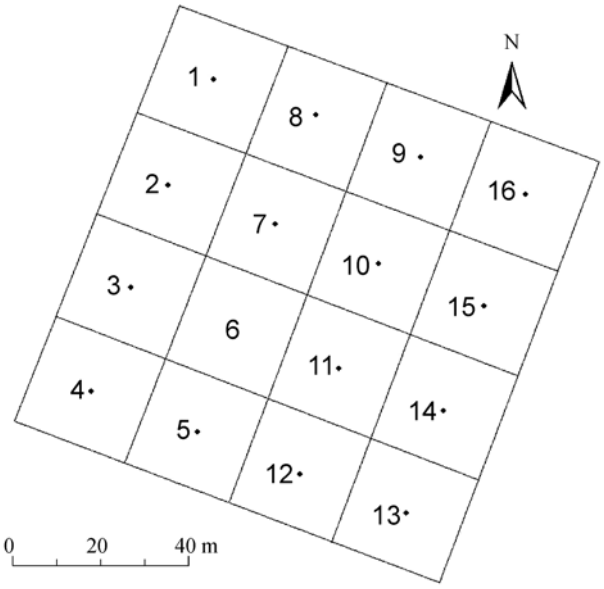

Figure 1 Positions of hemispherical photographs in plot.

3 Methods

3.1 Theory and background

In addition to LIDAR height information, most discrete LIDAR systems also record the intensity (sometimes referred to as the amplitude) of each received echo. The intensity represents the reflectance characteristics of the surface in the near infrared spectra between wavelengths of 800 and 1550 nm. LIDAR intensity is also an important information source which can be exploited in forest characterization. Many studies have used LIDAR intensity information to classify forest species[32−36]. Height and age-related differences in intensity correspond to both structural and compositional features of each stand, which has been demonstrated using global and local estimates of

spatial autocorrelation derived from LIDAR intensity information[37].

LIDAR intensity is influenced not only by reflectivity, moisture content, roughness, and other target surface properties, but also by the dynamic geometric relationship between sensor and target[32,37]. The dynamic sensor-target geometry includes the laser path length, which varies with the distance between the sensor and target; the orientation of the target relative to the sensor, which varies with the laser scan angle or topography; the footprint size, which varies with laser beam divergence; the attenuation in the atmosphere[32]. How each of these factors influences LIDAR intensity requires further investigation. The strength of these influences is unknown, but in an experimental situation, the impact of some of these factors may be decreased by making assumptions appropriate to the situation under study; the laser intensity returns are not affected when the scan angle is smaller than 10°[32]. So it may be assumed that the laser beam divergence and attenuation in the atmosphere in a given study area are constants during the same flight and the scan angle has no effects on the laser intensity. In this way, the interpretation of LIDAR intensity can be simplified.

Under the following assumptions[38]: 1) The entire footprint is reflected onto one surface (the extended target) and the target area A_s is circular, hence defined by the laser beam width β_t and the range R, and 2) the target has a solid angle of π steradians ($\Omega = 2\times\pi$ for scattering into a half sphere), the received laser power can be expressed in the following form[39]

$$P_r = \frac{P_t D_r^2 r}{R^4 b_t^2 W} \eta_{sys} \eta_{atm} A_s , \tag{1}$$

where P_r and P_t are the received and transmitted laser energy respectively, R is the distance between sensor and target, β_t is the laser-beam divergence, D_r is the diameter of the receiver aperture, Ω is the scattering solid angle of the target, ρ is the reflectivity of the target surface, A_s is the target area, and η_{sys} and η_{atm} are the system and atmospheric transmission factor respectively.

Eq. (1) represents the area of an extended diffuse target. The areas of non-extended diffuse targets show different range dependencies; for example, point targets (e.g., a leaf) with an area smaller than the footprint are range-independent[38]. Consequently, the received power reflected from point targets is represented by an inverse higher-order range-dependent function ($1/R^4$)

$$P_r = \frac{P_t D_r^2 \rho \mathrm{d}A}{4R^4 \beta_t^2} \eta_{sys} \eta_{atm} , \tag{2}$$

where dA is the area of the point target.

Let A_f be the area of the LIDAR footprint at the target elevation. Then the received signal power at the extended target and the point target can respectively be expressed as

$$P_{extended} = K \cdot \frac{\rho}{(4R)^2} , \tag{3}$$

$$P_{point} = K \cdot \frac{\rho}{(4R)^2} \cdot \frac{\mathrm{d}A}{A_f} , \tag{4}$$

where

$$K = P_t D_r^2 \eta_{sys} \eta_{atm} ,$$

$$A_f = \pi R^2 \beta_t^2 / 4 .$$

LIDAR intensity is the ratio of received to transmitted laser energy[37]. From Eqs. (3) and (4), it

is apparently found that the LIDAR intensity increases with the increasing reflectivity of the target and decreases with the decreasing distance between sensor and target. In a forested area, there are differences between vegetation and ground soil in both reflectivity and height. Because the reflectivity of vegetation is higher than that of ground soil at the 1064 nm wavelength and the elevation of vegetation is higher than that of the ground in a small local area, and the LIDAR intensity from vegetation should be higher than the intensity from ground, with the other things being equal. However, the intensity of the vegetation is actually much less than that of the ground. The reason is that the area of each point target (e.g., a needle leaf) is much smaller than the footprint area, that is the ratio of dA and A_f is much smaller than 1. Based on eqs. (3) and (4), the difference between P_{extented} and P_{points} can be thought to be large enough to discriminate. The result has been proved in some studies[14,26].

With such a theory, it is possible to separate almost all vegetation points from ground points, especially in conifer forest areas. After the separation of LIDAR points, digital terrain model and vegetation fractional cover were generated from ground points and vegetation points, respectively. The whole procedure for generation of DTM and vegetation fractional cover is illustrated in Figure 2.

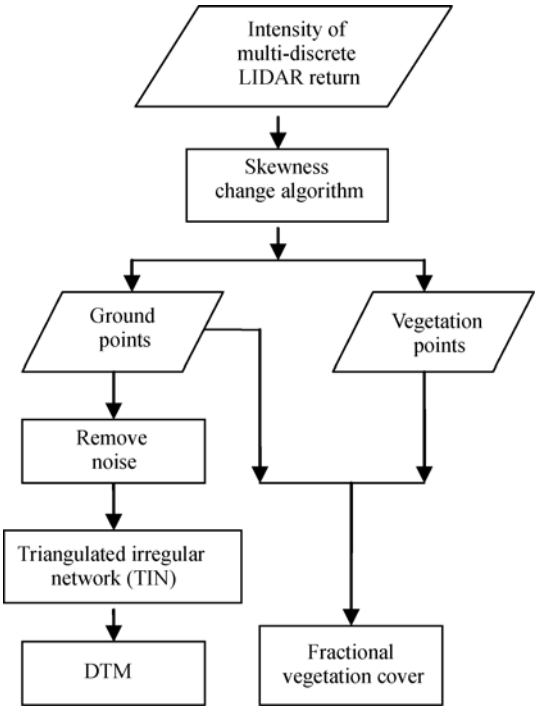

Figure 2 Flow chart of generation of DTM and vegetation fractional cover.

3.2 Separation of ground points and vegetation points

In this study, an approach based on LIDAR intensity information has been used to separate ground points from vegetation points in the LIDAR point cloud. Based on the central limit theorem, naturally measured samples will follow a normal distribution. The object points may disturb the normal distribution[13]. The statistical results of LIDAR intensity from several different area samples were used to prove the aforementioned assumption. Seen from Figure 3, its distribution of LIDAR intensity could look a combinatin with two normal distributions, no matter whether the

sample area is 50 m×50 m, or 100 m×100 m, or 200 m×200 m or 400 m×400 m. The skewness and kurtosis of this distribution are two characteristics, which were used in many statistical analyses that can be used to describe the distribution of LIDAR points based on its intensity. Based on the change curves of skewness and kurtosis, the vegetation points were separated from ground points. The details of the algorithm were described by Bao et al.[14].

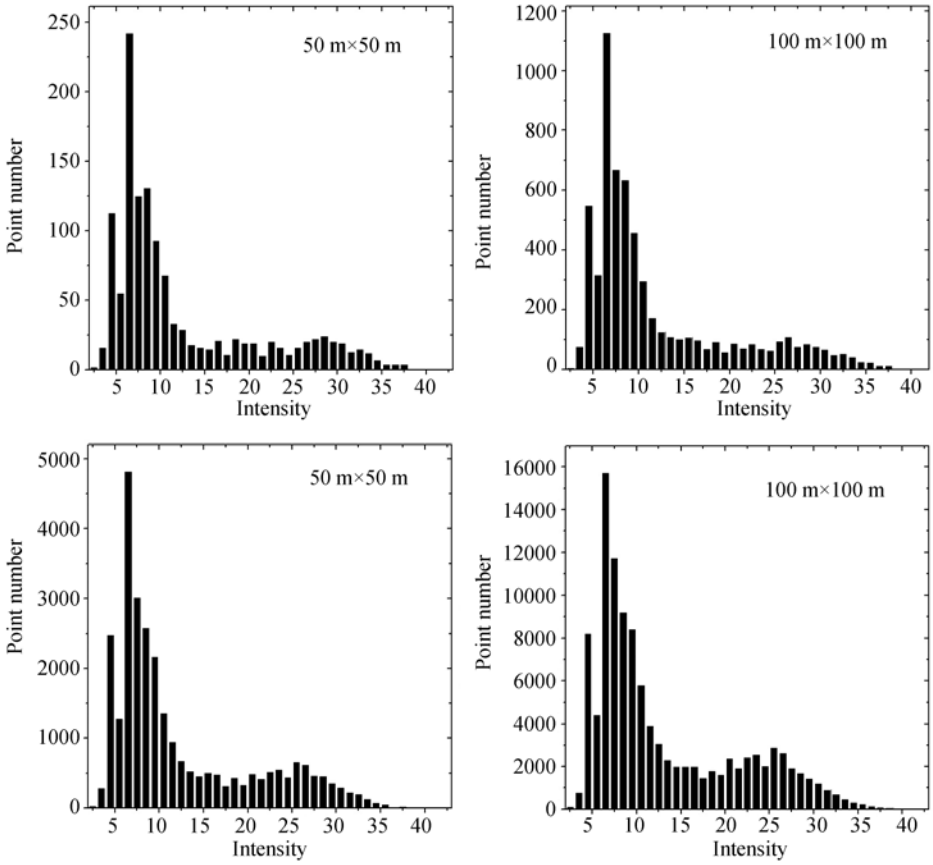

Figure 3 Distribution of LIDAR intensity from four different sample areas.

3.3 Generation of DTM

The ground points from LIDAR points calculated using skewness change algorithm still include a few above-ground points which are indicated as noise. After removing the noise, a digital terrain model (DTM) can be constructed from the ground points within a defined grid box[40]. First, a triangulated irregular network (TIN) can be constructed for the ground point based on a Delaunay triangulation of its elevation data. Then a rectangular grid of pixels is extracted from each TIN using linear interpolation with a constant sampling interval of one meter. Finally, the raster DTM of one-square-meter spatial resolution is generated.

3.4 Estimation of vegetation fractional cover

Separation of vegetation points and ground points is precondition of estimation of vegetation fractional cover. Previously, many studies used a first pulse, a last pulse, a single pulse or all of LIDAR data to derive vegetation fractional cover. Since most significant information is still con-

tained in a first pulse and separation of vegetation points and ground points is not explored, some stand level indices have been derived from only first pulse data[41]. But the vegetation fractional cover from the first pulse data is larger than that from single pulse, which in turn is larger than that from last pulse data[19,28]. In our study, because five flights were carried out, the same point may be found in different flight. For avoiding the repetitive calculation of the same point in the estimation of vegetation fractional cover, redundant points in the same position could be removed. After separation of vegetation points and ground points using the approach in this study, vegetation fractional cover is easily computed from eq. (5),

$$f_{\text{cover}} = \frac{\sum E_{\text{vegetation}}}{\sum E_{\text{total}}}. \tag{5}$$

4 Results

4.1 Separation of ground points and vegetation points

After the laser intensity data are processed with the skewness change algorithm, ground points and vegetation points can be effectively separated. As showed in Figure 4(a), the green points denote the separated above-ground vegetation points and the yellow points denote the ground points. Figures 4(b) and (c) present the profiles of map 4(a) in direction of north-south and east-west, respectively. As seen from Figures 4(b) and (c), a few vegetation points are classified into ground points, but a few of ground points are classified into vegetation points. This may be effect on estimation of fractional vegetation cover, which would be introduced in Section 4.3.

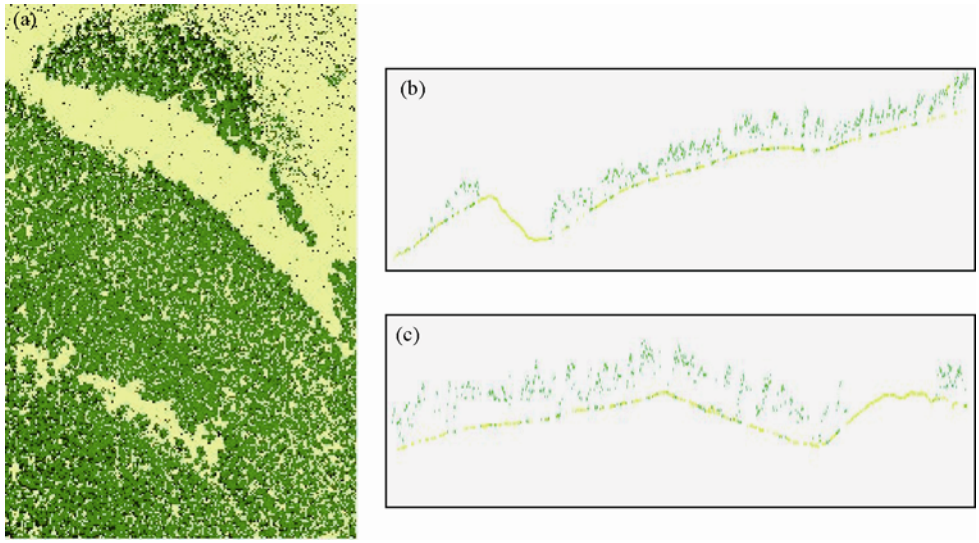

Figure 4 Map of separation of ground points and vegetation points (The green points denote the vegetation points; the yellow points denote the ground points; the black points denote the area without laser points; (b) and (c) are profiles of map (a) in direction of north-south and east-west, respectively).

4.2 Validation of DTM

To assess the overall performance of the proposed algorithm and the given laser scanner data, the DTM computed with the proposed algorithm was compared with the points measured with total station. Compared with 1546 field measurements, the extremes of their difference are −95.1 and

+94.8 cm, the mean value is −18.5 cm and the RMSE (root mean square error) is ±20.9 cm. As showed in Figure 5, the difference between field measurements and laser scanner data leads to a normal distribution. The residual of −18.5 cm indicates that the DTM from the laser points is lower than that from field measurements. The possible reason is that most of positions of the field measurements are lie under trees and only a few of laser points lie on ground under the trees, which affect the values of DTM from laser scanner data.

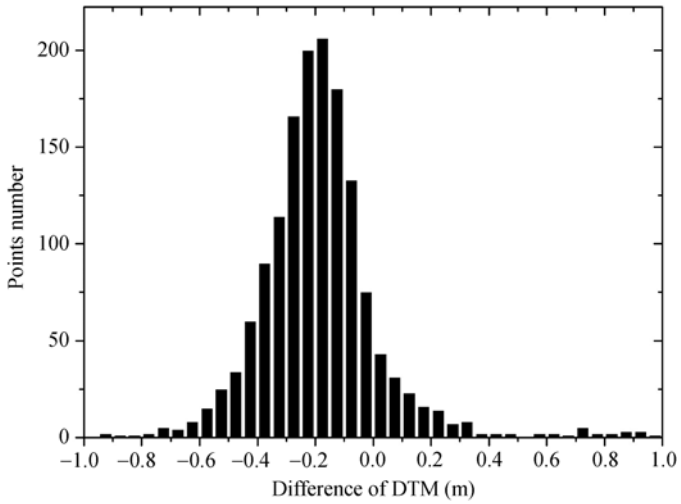

Figure 5 Distribution of difference between laser scanner data and field measurements.

4.3 Estimation of vegetation fractional cover

According to the thesis[42], the innermost zenith angles up to 10° should be used for the derivation of vegetation fractional cover from hemispherical photographs. Additionally, the data trap sizes of radii up to 2 m have the highest correlation with the zenith angles up to 10°[19]. So the data trap sizes of 4 m in diameter from airborne laser scanner data were selected to compute vegetation fraction cover. As showed in Figure 6, the R^2 for the regression of fractional vegetation cover from

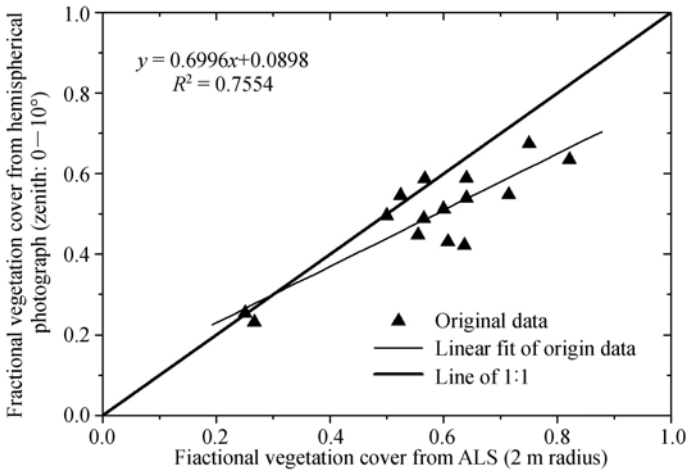

Figure 6 Regression of fractional vegetation cover derived from airborne laser scanner data with respective values from hemispherical photographs.

these ALS data and the respective field measurements is 0.7554. Additionally, the fractional vegetation cover from the ALS data is higher than the corresponding parameter from hemispherical photographs. There are two possible reasons: one is that some ground points are classified into vegetation points during the separation, and the other is that less energy of laser leads to less density of ground points in dense forested area.

5 Conclusions

The airborne laser scanner data are becoming popular for the generation of DTM and estimation of forest stand parameters, such as tree height, crown size, fractional vegetation cover, and LAI. For a discrete return of laser scanner data, point cloud needs to be classified for abovementioned parameters. For DTM and forest structure parameters, they were separately retrieved from laser scanner data in previous study, as the separation of ground points from vegetation points in forested area are not easy. We proposed an algorithm for separation of ground points and vegetation points, so the DTM and fractional vegetation cover can be estimated synchronously after the separation. This study is to evaluate the potential of the algorithm for deriving DTM and fractional vegetation cover.

This method is based on LIDAR intensity information and theoretical considerations about the interaction of the laser beam with different targets. According to the distribution of the intensity of laser scanner data, the points of ground and vegetation in forested area belong to two normal distributions, respectively. We use the skewness change of the intensity to separate the two distributions. That is, the laser scanner data can be classified into ground points and vegetation points using the skewness change algorithm. The DTM and fractional vegetation cover can be estimated from separation of ground points and vegetation points. Although most of ground points and vegetation points could be separated, a few vegetation points still remain in ground points. And the residual vegetation points are removed as noise from the ground points before generating the DTM. For validating the estimation of the DTM, 1546 field measurements of total stations in test area are selected. The extremes of their difference are −95.1 and +94.8 cm, the mean value is −18.5 cm and the RMSE is ±20.9 cm. We have found that the DTM from laser scanner data in sloped forested area is lower than that from field measurements. The results can be explained by the measurements characteristics of laser scanning. The fractional vegetation cover is estimated using the vegetation points separated from laser scanner data. Compared with the hemispherical photographs, the R^2 of the regression is up to 0.7554. Additionally, we could find the fractional vegetation cover from the ALS data is higher than the corresponding parameter from hemispherical photographs. Some ground points are classified into the vegetation points, which resulting in more vegetation points. The other possible reason is that the higher fight causes less laser energy, which causes the less density of ground points. Other error sources are not excluded absolutely. The processing of hemispherical photographs involves the process of manually threshold images, which is a potential source for biases and random noise.

In future work, the algorithm would be tested in other different vegetation types. And the ground points which are classified into vegetation points should be separated from them for high accuracy estimation of fractional vegetation cover. From these vegetation points, some forest structure parameters can be also estimated, such as LAI. The first and last returns of the airborne laser scanner data have been used to estimate the LAI and regression of the ALS estimates with field meas-

urements showed moderate to good agreement[19]. Combined with the TLS (terrestrial laser scanner) data, the airborne laser scanner data can be used to retrieve a map of high accuracy LAI. This combination of the ALS and TLS will be a subject of our future work. Additionally, we also study how the specific parameters of the ALS and TLS effect the estimation of forest stand parameters.

1 Bonan G B. Importance of leaf area index and forest type when estimating photosynthesis in boreal forests. Remote Sens Environ, 1993, 43(3): 303－314
2 Li Q Q, Wang Z, Yang B S. Multi-resolution representation of digital terrain models with terrain features preservation (in Chinese). Sci China Ser E-Tech Sci, 2008, 51(Suppl): 145－154
3 Kraus K, Pfeifer N. Determination of terrain models in wooded areas with airborne laser scanner data. ISPRS J Photogramm Remote Sens, 1998, 53(4): 193－203
4 Axelsson P. DEM generation from laser scanner data using adaptive TIN models. In: International Archives of Photogrammetry and Remote Sensing. Istanbul: ISPRS, 2000. 110－117
5 Kilian J, Haala N, Englich M. Capture and evaluation of airborne laser data. In: International Archives of Photogrammetry and Remote Sensing. Vienna: ISPRS, 1996. 383－388
6 Vosselman G. Slope-based filtering of laser altimetry data. In: International Archives of Photogrammetry and Remote Sensing, Amsterdam, Netherlands: GITC, 2000. 935－942. http://www.itc.nl/personal/vosselman/papers/vosselman2000.adam.pdf
7 Zhang K, Chen S C, Whitman D, et al. A progressive morphological filter for removing non-ground measurements from airborne LIDAR data. IEEE Trans Geosci Remote Sens, 2003, 41(4): 872－882
8 Chen Q, Gong P, Baldocchl D, et al. Filtering airborne laser scanning data with morphological methods. Photogramm Eng Remote Sens, 2007, 73(2): 175－185
9 Elmqvist M, Jungert E, Lantz F, et al. Terrain modeling and analysis using laser scanner data. In: Michelle A H, eds. Proceedings of the ISPRS Workshop "Land Surface Mapping And Characterization Using Laser Altimetry". Annapolis MD: ISPRS, 2001. 219－226
10 Akel N A, Zilberstein O, Doytsher Y. Automatic DTM extraction from dense raw LIDAR data in urban areas. In: Proceedings, International Federation of Surveyors (FIG) Working Week 2003, Paris, France, 2003. 1－10. http://www.fig.net/pub/fig_2003/TS_26/PP26_1_AboAkel_et_al.pdf
11 Krzystek P. Filtering of laser scanning data in forest areas using finite elements. In: 3-D Reconstruction from Airborne Laser Scanner and InSAR Data. Dresden: ISPRS, 2003. http://www.isprs.org/commission3/wg3/workshop-laserscanning/(accessed October 18, 2007)
12 Kobler A, Pfeifer N, Ogrinc P, et al. Repetitive interpolation: A robust algorithm for DTM generation from aerial laser scanner data in forested terrain. Remote Sens Environ, 2007, 108(1): 9－23
13 Bartels M, Wei H, Mason D C. DTM generation from LIDAR data using skewness balancing. In: Tang Y Y, Wang S P, Lorette G, et al, eds. Proceedings, 18th International Conference on Pattern Recognition. Part I. Hong Kong, China: IEEE Computer Society Press, 2006. 566－569
14 Bao Y F, Li G P, Cao C X, et al. Classification of LIDAR point cloud and generation of DTM from LIDAR height and intensity data in forested data. In: George V, Chen J, Mir A M, et al, eds. The International Archives of the Photogrammetry, Remote Sensing and Spatial Information Sciences. Beijing: ISPRS, 2008. 313－318
15 Cohen W B, Maiersperger T K, Gower S T, et al. An improved strategy for regression of biophysical variables and landsat etm+ data. Remote Sens Environ, 2003, 84(4): 561－571
16 Colombo R, Bellingeri D, Fasolini D, et al. Retrieval of leaf area index in different vegetation types using high resolution satellite data. Remote Sens Environ, 2003, 86(1): 120－131
17 Koetz B, Schaepma M, Morsdorf F, et al. Radiative transfer modeling within a heterogeneous canopy for estimation of forest fire fuel properties. Remote Sens Environ, 2004, 92(3): 332－344
18 Schlerf M, Atzberger C. Inversion of a forest reflectance model to estimate structural canopy variables from hyperspectral remote sensing data. Remote Sens Environ, 2006, 100(3): 281－294
19 Morsdorf F, Kötz B, Meier E, et al. Estimation of LAI and fractional cover from small footprint airborne laser scanning data based on gap fraction. Remote Sens Environ, 2006, 104(1): 50－61

20 David L A G, Ross A H. Quantifying canopy height underestimation by laser pulse penetration in small-footprint airborne laser scanning data. Can J Remote Sens, 2003, 29(5): 650－657
21 Harding D J, Lefsky M A, Parker G G, et al. Laser altimeter canopy height profiles: Methods and validation for closed canopy, broadleaf forests. Remote Sens Environ, 2001, 76(3): 283－297
22 Hollaus M, Wagner W, Maier B, et al. Airborne laser scanning of forest stem volume in a mountainous environment. Sensors, 2007, 7(8): 1559－1577
23 Lefsky M A, Harding D, Cohen W B, et al. Surface LiDAR remote sensing of basal area and biomass in deciduous forests of Eastern Maryland, USA. Remote Sens Environ, 1999, 67(1): 83－98
24 Lefsky M A, Cohen W B, Acker S A, et al. Lidar remote sensing of the canopy structure and biophysical properties of Douglas-fir western hemlock forests. Remote Sens Environ, 1999, 70(3): 339－361
25 Magnussen S, Boudewyn P. Derivations of stand heights from airborne laser scanner data with canopy-based quantile estimators. Can J For Res, 1998, 28(7): 1016－1031
26 Wagner W, Hollaus M, Briese C, et al. 3D vegetation mapping using small-footprint full-waveform airborne laser scanners. Int J Remote Sens, 2008, 29(5): 1433－1452
27 White M A, Asner G P, Nemani R R, et al. Measuring fractional cover and leaf area index in arid ecosystems: Digital camera, radiation transmittance, and laser altimetry results. Remote Sens Environ, 2000, 74(1): 45－57
28 Lovell J, Jupp D, Culvenor D, et al. Using airborne and groundbased ranging lidar to measure canopy structure in Australian forests. Can J Remote Sens, 2003, 29(5): 607－622
29 Riano D, Valladares F, Condes S, et al. Estimation of leaf area index and covered ground from airborne laser scanner (lidar) in two contrasting forests. Agric For Meteorol, 2004, 124(3-4): 269－275
30 Koetz B, Morsdorf F, Sun G, et al. Inversion of a lidar waveform model for forest biophysical parameter estimation. IEEE T Geosci Remote Lett, 2006, 3(1): 49－53
31 Frazer G W, Canham C D, Lertzman K P. Gap light analyzer (GLA), Version 2.0: Image-processing software to analyze true-color, hemispherical canopy photographs. Bull Ecol Soc Amer, 2000, 81: 191－197
32 Donoghue D N M, Watt P J, Cox N J, et al. Remote sensing of species mixtures in conifer plantations using LIDAR height and intensity data. Remote Sens Environ, 2007, 110(4): 509－522
33 Holmgren J, Persson Å. Identifying species of individual trees using airborne laser scanning. Remote Sens Environ, 2003, 90(4): 415－423
34 Moffiet T, Mengersen K, Witte C, et al. Airborne laser scanning: Exploratory data analysis indicates potential variables for classification of individual trees or forest stands according to species. ISPRS J Photogramm Remote Sens, 2005, 59(5): 289－309
35 Ørka H O, Næsset E, Bollandsås O M. Utilizing airborne laser intensity for tree species classification. In: Rönnholm P, Hyyppä H, Hyyppä J. Proceedings of the ISPRS Workshop "Laser Scanning 2007 and SilviLaser 2007". Espoo: ISPRS, 2007. 300－304
36 Schreier H, Lougheed J, Tucher C, et al. Automated measurements of terrain reflection and height variations using an airborne infrared laser system. Int J Remote Sens, 1985, 6(1): 101－113
37 Langford J, Niemann O, Frazer G, et al. Exploring small footprint LIDAR intensity data in a forested environment. In: Proceedings, IEEE International Conference on Geoscience and Remote Sensing Symposium. Denver: IEEE, 2006. 2416－2419
38 Höfle B, Pfeifer N. Correction of laser scanning intensity data: Data and model-driven approaches. ISPRS J Photogramm Remote Sens, 2007, 62(6): 415－433
39 Wagner W, Ullrich A, Ducic V, et al. Gaussian decomposition and calibration of novel small-footprint full-waveform digitising airborne laser scanner. ISPRS J Photogramm Remote Sens, 2006, 60(2): 100－112
40 Hollaus M, Wanger W, Eberhöfer C, et al. Accuracy of large-scale heights derived from LIDAR data under operational constraints in a complex alpine environment. ISPRS J Photogramm Remote Sens, 2006, 60(5): 323－338
41 Yu X, Hyypä J, Kaartinen H, et al. Automatic detection of harvested trees and determination of forest growth using airborne laser scanning. Remote Sens Environ, 2004, 90(4): 451－462
42 Weiss M, Baret F, Smith G J, et al. Review of methods for in situ leaf area index (LAI) determination: Part II. Estimation of LAI, errors and sampling. Agric For Meteorol, 2004, 121(1-2): 37－53